Journal of Organometallic Chemistry 924 (2020) 121462

Contents lists available at ScienceDirect

Journal of Organometallic Chemistry

journal homepage: www.elsevier.com/locate/jorganchem

Theoretical insights into the electronic structure of nickel(0)-diphosphine-carbon dioxide complexes

Tímea R. Kégl [a,b,c], Rui M. B. Carrilho [d], Tamás Kégl [a,b,c,*]

[a] Department of Inorganic Chemistry, University of Pécs, Ifjúság útja 6., H-7624 Hungary
[b] János Szentágothai Research Centre, Pécs, Ifjúság útja 34., H-7624 Hungary
[c] MTA-PTE Research Group for Selective Chemical Syntheses, Hungary
[d] University of Coimbra, Coimbra Chemistry Centre, Department of Chemistry Rua Larga, Coimbra 3004-535, Portugal

ARTICLE INFO

Article history:
Received 30 June 2020
Revised 22 July 2020
Accepted 25 July 2020
Available online 26 July 2020

Keywords:
Nickel(0)
Carbon dioxide complexes
QTAIM
DAFH
EDA-NOCV

ABSTRACT

The coordination properties of carbon dioxide bound to Ni(0) with various phosphines have been investigated by means of DFT calculations. Reasonable linear correlation has been found between Tolman's electronic parameters (TEPs) and the asymmetric stretching frequency of the coordinated CO_2. Two descriptors from EDA-NOCV calculations, namely the interaction energy and the Hirshfeld charge associated with the back donation component gave acceptable linear correlation as well with the TEPs. The coordination strength, as well as the C=O bond order in coordinated carbon dioxide can be tuned by varying the substituents on phosphorus: in the presence of electron withdrawing groups the C=O bond remains stronger and Ni-C interaction is weaker, moreover, a new Ni-O bond path is formed; whereas for more basic diphosphines the Ni–C bond order is higher and the coordinated carbon dioxide possess a weaker C=O bond.

1. Introduction

Carbon dioxide is considered an ubiquitous C1 building block since it is an inexpensive, non-flammable, and highly abundant carbon source [1,2]. Although CO_2 is currently used in a number of industrial processes, it remains a molecule with low reactivity, due to both intrinsic thermodynamic and kinetic issues [3,4]. Therefore, the development of efficient methodologies for its activation and chemical fixation are topics of utmost interest and still constitute some of the greatest challenges for both the chemical industry and academy [5,6]. A promising approach toward CO_2 activation is offered by coordination to transition metal complexes, since it lowers the activation energy, making possible to convert this "inert" molecule into a plethora of value-added products [7]. The interaction of CO_2 with transition metal complexes has been the subject of extensive studies [8–10], both experimental and theoretical. Furthermore, in the last decade, a number of transition metal complexes have been reported as efficient catalysts for a variety of CO_2 transformations [11,12], such as CO_2 reduction [13,14], copolymerization reactions through coupling with epoxides [15,16] and CO_2 hydrogenation to olefins [17], among other.

Phosphines, phosphites, and other P-donor ligands are of crucial importance in the most reactions catalyzed by transition metal (TM) compounds. Changing the coordinated ligands is a straightforward strategy for 'fine-tuning' the properties of transition metal containing catalysts. The catalytic properties of transition-metal complexes, such as their activity, are principally determined by the steric and electronic properties of the ligands bound to the metal. The structural variation of the spectator ligands opens the possibility to tune the catalytic activity, as well as chemo-, regio-, and enantioselectivity. It has long been known that altering the substituents on the phosphorus atom can cause changes upon coordination in the geometry and electronic structure of the ligands as well as their TM complexes. The nature of the transition metal–phosphorus bond and its influence on the other bonds in the molecule provide crucial information for the characterization of catalytically active compounds and for the optimization of their properties in order to develop more efficient catalysts.

In their seminal work, Strohmeier et al. studied the σ-donor and π-acceptor properties of various types of ligands, such as nitriles, isonitriles, sulfoxides, and phosphines. The phosphines were further separated into four categories designated from I to IV,

* Corresponding author at: Department of Inorganic Chemistry, University of Pécs, Ifjúság útja 6., H-7624 Hungary.
E-mail address: tkegl@gamma.ttk.pte.hu (T. Kégl).

https://doi.org/10.1016/j.jorganchem.2020.121462

classified by frequency regions. They were sorted by wavenumber into increasing order [18]. These classes served as the basis for Tolman's famous formula.

First, in 1970, Tolman reported the A_1 carbonyl stretching frequencies of $NiL(CO)_3$ complexes, with monodentate P-donor ligands ($L = PR^1R^2R^3$) [19,20] comparing the electronic effects of 70 phosphorus-containing ligands. It was established that a contribution could be assigned to each substituent on phosphorus and the sum of those contributions was equal to the entire influence of the ligand on the symmetric carbonyl stretching frequency ν(CO). This contribution was designated as χ_i (cm^{-1}), and the most basic ligand (tri-*tert*-butylphosphine) was chosen as a reference on the TEP (the Tolman electronic parameter) scale recognizing that P^tBu_3 is the best σ-donor and the worst π-acceptor ligand (Eq. (1)). The $NiL(CO)_3$ scale, that is the TEP, correlates well with Strohmeier's $CpMnL(CO)_2$ system [21,22] (Eq. (2)).

$$\nu(CO)_{Ni} = 2056.1 + \Sigma\chi_j \quad (1)$$

$$\nu(CO)_{Ni} = 0.711 \cdot \nu(CO)_{Mn} + 692 \quad (cm^{-1}) \qquad R = 0.970 \quad (2)$$

Chelating ligands, such as diphosphines, however, cannot be characterized within the framework of the TEP scale. Crabtree et al. suggested more appropriate model complexes for chelating ligands, for example, $MoL_2(CO)_4$ (L_2: bidentate phosphine ligand or two monodentate phosphines) [23]. They compared 11 P donor ligands of various types and correlated to the existing TEP scale using Eq. (3). Thus, Crabtree proved Tolman's statement that the choice of transition metal carbonyl system is arbitrary and interchangeable.

$$\nu(CO)_{Ni} = 0.593 \cdot \nu(CO)_{Mo} + 871 \qquad R = 0.996 \quad (3)$$

Otto and Roodt established a simple quadratic equation for the Rh-Vaska complexes and $NiL(CO)_3$ [24]. Later, the relationship between the carbonyl stretching frequencies of the two reference complexes was revised, and the ν(CO) range was divided into two sections depending on the basicities of the ligands. The slope for the more basic phosphines showed a difference to those possessing less basicity.

In recent decades, several attempts have been made for finding theoretical methods for the appropriate description of the donor and acceptor properties of ligands. The first group of methods deals only with the isolated ligand, focusing on its electronic and steric properties. The molecular electrostatic potential at the lone pair of the phosphorus atom should be mentioned, which correlates reasonably well with the TEP scale, according to Suresh and Koga [25], which should be first mentioned as a prominent example. Quantitative analysis of ligand effects (QALE) relies on experimental data of known ligands and provides the resolution of net donating ability into QALE parameters [26,27]. The second category focuses on entire transition metal complexes thereby include the possibility to scrutinize interligand effects as well [28]. Various electronic structure methods, such as the Extended Transition State theory combined with the Natural Orbitals of Chemical Valence (ETS-NOCV also denoted as EDA-NOCV) [29–32] and QTAIM (Quantum Theory of Atoms in Molecules) [31] have been employed as well. The CEP, that is the computationally derived ligand electronic parameter, based on vibrational frequencies, was investigated by Crabtree and co-workers [33].

Although the TEP scale achieved a widely accepted status, its limitations should be mentioned as well. The coordinating properties of a ligand are governed by its σ-donor and π-acceptor abilities together, whereas TEP (or CEP) only gives the *net* donor strength. Moreover, secondary interactions, like through-space ligand interactions, may affect the carbonyl stretching frequencies as reported by Sierra and co-workers for manganese half-sandwich

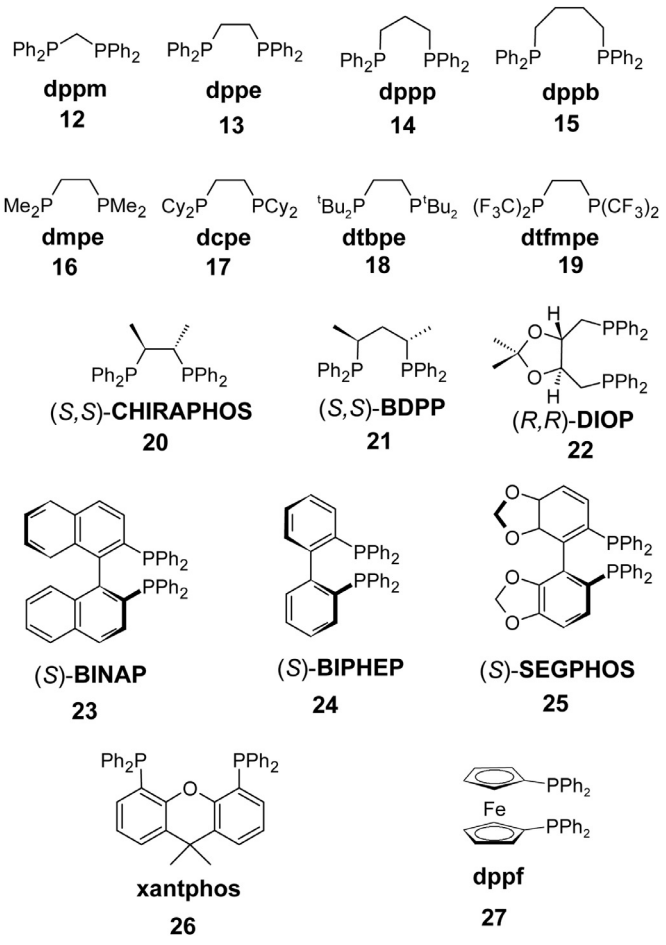

Fig. 1. Chelating phosphines considered in this study.

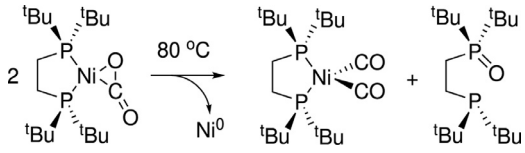

Fig. 2. Stoichiometric reduction of carbon dioxide according to Hillhouse et al.[36].

complexes [34]. Moreover, it was also reported that the Tolman electronic parameters failed for linear Au-carbonyl complexes [35].

The goal of this computational study is to establish a relationship between the ligand electronic effects of nickel(0)-phosphine-carbon dioxide complexes with the Tolman's scale, that is, the totalsymmetric carbonyl stretching frequencies of $Ni(CO)_3L$ complexes thereby providing a direct comparison of the electronic effects of diphosphines and monophosphines. By the selection of appropriate ligands the set of ligands, employed by Crabtree [23] and Tolman [19], has been adopted, that is PEt_3 (**1**), PEt_2Ph (**2**), PMe_3 (**3**), PMe_2Ph (**4**), PPh_3 (**5**), $P(OMe)_3$ (**6**), $P(OMh)_3$ (**7**), $PCl_2(OEt)$ (**8**), PCl_3 (**9**), PF_3 (**10**), and $PF_2(CF_3)$ (**11**). The diphosphines that are investigated in this study are depicted in Fig. 1.

The second goal of this work to investigate the inherent electronic properties of the coordinated carbon dioxide, keeping in perspective its catalytic applications. Changing the coordination strength, or decreasing the O–C bond order to the desired level might lead to feasible catalytic or stoichiometric reactions that utilize carbon dioxide. A notable example, reported by Hillhouse and co-workers, is complex $Ni(dtbpe)(CO_2)$ that can reduce CO_2 to CO in the presence of carbon dioxide [36] (Fig. 2).

Table 1
Experimental CO stretching frequencies (Ref[19].) for $NiL(CO)_3$; computed CO_2 stretching frequencies; Ni-C and O1-C distances for $NiL_2(CO_2)$ complexes at the PBEPBE level of theory. O1 denotes the oxygen atom being involved in the η^2-(C,C) coordination.

Ligand	$\nu(CO)_{NiL}(CO)_3$ [cm^{-1}]	$\nu(CO_2)_{NiL_2(CO_2)}$ [cm^{-1}]	r(Ni-C) [Å]	r(O1-C) [Å]
PEt_3 (**1**)	2061.7	1827	1.884	1.271
PEt_2Ph (**2**)	2063.7	1846	1.899	1.268
PMe_3 (**3**)	2064.1	1832	1.885	1.267
PMe_2Ph (**4**)	2065.3	1827	1.884	1.268
PPh_3 (**5**)	2068.9	1855	1.906	1.264
$P(OMe)_3$ (**6**)	2079.5	1856	1.937	1.267
$P(OMh)_3$ (**7**)	2085.3	1877	1.929	1.258
$PCl_2(OEt)$(**8**)	2092.5	1964	1.966	1.250
PCl_3(**9**)	2097.0	1997	1.993	1.244
PF_3 (**10**)	2110.8	2005	2.005	1.243
$P(CF_3)F_2$ (**11**)	2112.1	2024	2.024	1.240

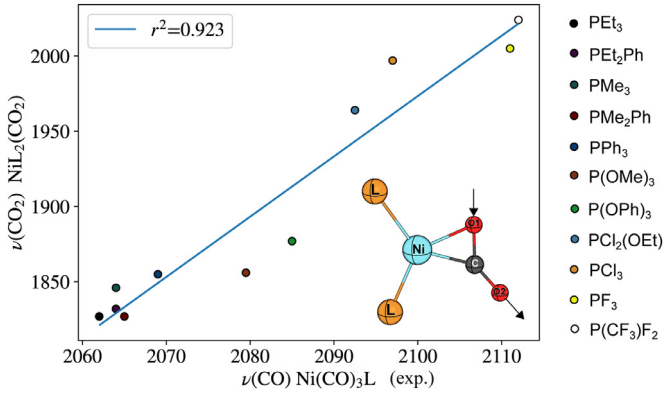

Fig. 3. Relationship between the experimental Tolman's parameters and the computed asymmetric CO_2 stretching frequencies in complexes $NiL_2(CO_2)$.

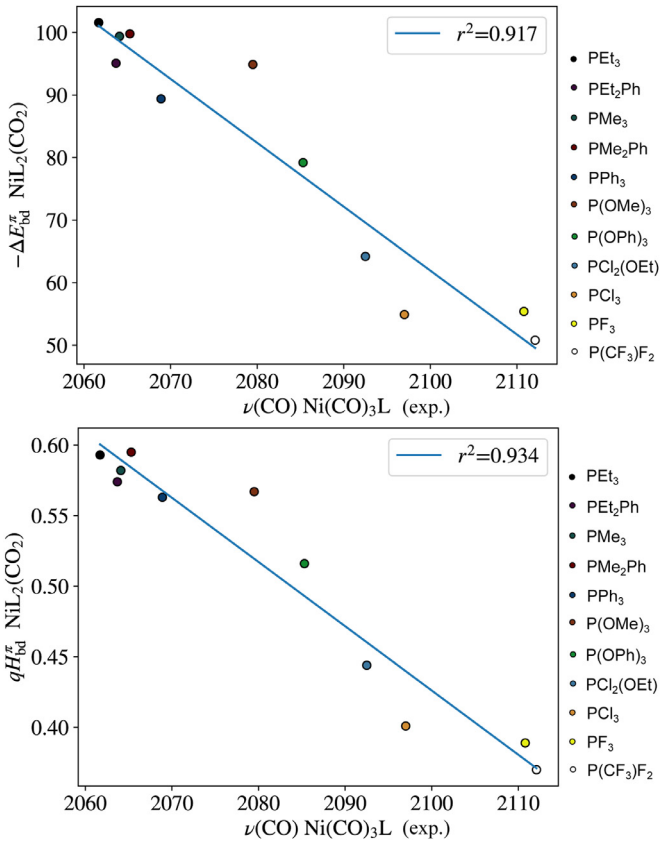

Fig. 4. Relationship between the experimental Tolman's parameters and the EDA-NOCV related parameters associated with back donation in complexes $NiL_2(CO_2)$: the orbital energy ΔE^{π}_{bd} (top) and the Hirshfeld charge component qH^{π}_{bd} (bottom). Vibrational frequencies are given in cm^{-1}.

2. Computational details

All the structures were optimized without symmetry constraints with tight convergence criteria using the Gaussian suite of programs [37] with the exchange and correlation functionals developed by Perdew, Burke, and Ernzherhof [38] and denoted as PBEPBE. For all the atoms the def2-TZVP basis set [39] was employed. For the complexes containing conformationally flexible ligands, conformational analyses have been performed in a similar manner reported earlier [31] and the lowest energy species were considered. QTAIM (Quantum Theory of Atoms In Molecules) analyses of the wave function [40] were carried out with the AIMAll software [41]. For the EDA-NOCV calculations, the ADF 2019 software was used [42] employing the PBEPBE functional in combination with the triple-ζ STO basis set for all atoms with one set of polarization functions (denoted as TZP) and a small frozen core.

3. Results and discussion

In Table 1, the $\nu(CO_2)$ parameters are collected for various phosphorus ligands, which had also been used by Crabtree et al. In Fig. 3, the 11 carbonyl stretching frequencies of the training set of $NiL_2(CO_2)$ species are illustrated depending on $NiL(CO)_3$ values. The acceptable value of the correlation coefficient ($r^2 = 0.923$) shows that the computed $\nu(CO_2)$ values in $NiL_2(CO_2)$ complexes have a reasonable linear correlation with experimental $\nu(CO)_{Ni}$ according to Eq. 4:

$$TEP = CEP_{CO_2} = 0.23034 \cdot \nu(CO_2) + 1644.1 \quad (4)$$

As a general trend, the Ni-C distance decreases and the O1–C bond (where O1 is the oxygen atom being involved in the η^2-(C,C) coordination) length increases upon the increase of the phosphine basicity, in line with the decreasing $\nu(CO_2)$ as the back donation is expected to become more and more dominant.

It was reported earlier by us [31] that the bonding energy component, within the framework of the EDA-NOCV methodology, for the donor interaction in complexes $Ni(CO)_3$(monophosphine) shows a reasonable correlation with Tolman's electronic parameters. Chen and co-workers pointed out that the correlation is less linear when other monodentate ligands are included in the training set [32]. They showed, however, that the Hirshfeld charge divided into components, according to the deformation density contributions, is a better indicator for the electronic parameter of monodentate ligands.

For the Ni(0)-CO_2 complexes, the deformation density component, related to back donation, had been anticipated to be the most informative component for the description of the electronic effect of phosphines. With the same training set as for Table 1. The orbital energy component (ΔE^{π}_{bd}) and the Hirshfeld charge associated with the back donation (qH^{π}_{bd}) were compared with the experimental Tolman electronic parameters. Both descriptors correlate well, with $r^2 = 0.917$ and $r^2 = 0.934$ for ΔE^{π}_{bd} and qH^{π}_{bd}, respectively, according to Eqs. 5 and 6 (see Fig. 4):

$$TEP = -0.89674 \cdot \Delta E^{\pi}_{bd} + 2154.0 \quad (5)$$

$$TEP = -205.27 \cdot qH^{\pi}_{bd} + 2186.3 \quad (6)$$

To shed some light on the coordination properties of carbon dioxide in the function of the basicity of the diphosphine EDA-NOCV calculations were carried out on complexes Ni(dmpe)(CO_2)

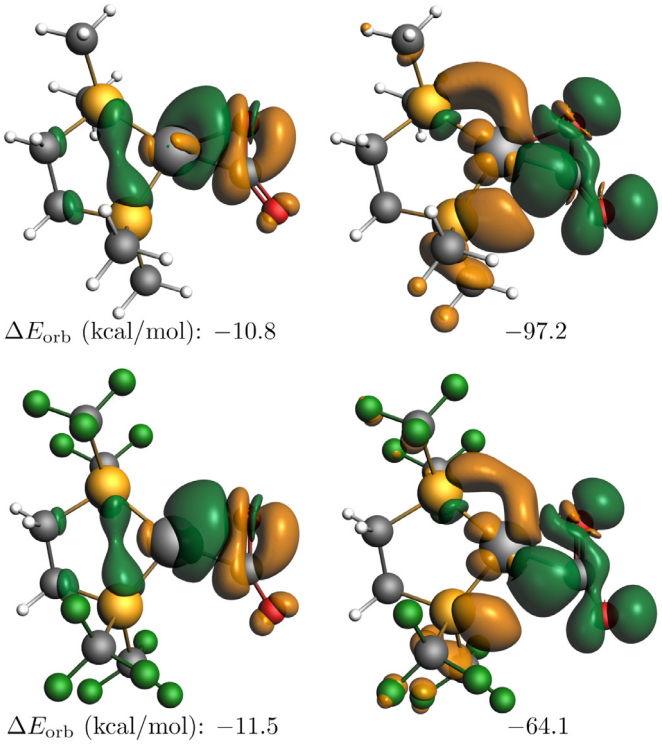

Fig. 5. Deformation density contributions in complexes $NiL_2(CO_2)$. The direction of the charge flow is indicated by the isosurface colors gold ($\Delta\rho < 0$) to green ($\Delta\rho > 0$), or lighter to darker. (For interpretation of the references to colour in this figure legend, the reader is referred to the web version of this article.)

and Ni(dtfmpe)(CO_2). EDA-NOCV is a particularly appropriate method for describing the bonding situation between ligands and the central atom in transition metal complexes. When the orbital interaction part is expressed in NOCV's, only a few complementary pairs will contribute to the interaction energy to a significant extent. The deformation density plots ($\Delta\rho_{\text{orb}}$) provide an appealing depiction of the direction of the charge flow taking place upon the coordination [29,30,43–46]. In our case, the two interacting fragments are Ni^0L_2 containing the metal center and CO_2 as the ligand.

The dominant deformation density contributions to donation and back donation are shown in Fig. 5 for two complexes with large difference in diphosphine basicities. By visual inspection, minor differences can be observed in the shape of isosurfaces of the dominant deformation density contributions. The difference in the energy component is a mere 0.7 kcal/mol for donation, in favor of the dtfmpe complex. As the total orbital interaction component is - 122.8 and - 87.5 kcal/mol in the presence of dmpe and dtfmpe, respectively, the orbital energy component for the back donation is expected to be lower for the electron withdrawing case. For the Ni(dtfmpe)(CO_2) complex, the energy component is by 33.1 kcal/mol lower than that for Ni(dmpe)(CO_2), thus the weaker interaction caused by the electron withdrawing character of the dtfmpe ligand is manifested in the weaker Ni-CO_2 backbonding.

The electronic structure analysis based on Domain Averaged Fermi Holes provides further insight into the nature of dominant donor-acceptor interactions between the ligand and the metal center. The DAFH concept, introduced by Ponec [47,48], is particularly suitable for analyzing non-obvious bonding situations [49–52]. The DAFH eigenvectors provide useful information about electron pairs; how they are shared between the two fragments. The sum of the eigenvalues of the complementary eigenvectors is close to 2.0, as they represent an electron pair, thus, the complementary eigenvalues can be transformed into percentages about the pair distributions between the fragments. Moreover, it is capable of giving a highly visual description of the bonding in classical terms of bonds, dangling valences, and lone pairs. It was previously shown for the simple model compounds $M(PH_3)_2(CO_2)$ (M = Ni,Pd,Pt) that the electron donation from the CO_2 fragment to the metal-based fragment stems from an in-plane π-type orbital that is based mostly on the in-plane *p*-orbital of the coordinating oxygen atom (O1) [53,54]. The back donation from the metal to CO_2 can be interpreted as a broken valence M–C σ bond based mainly on the $d_{x^2-y^2}$ orbital of the metal. A second type of back donation was also reported, that bypasses the metal center. In this case, the donor-acceptor interaction takes place between the depleted carbon as acceptor and the lone pair of the adjacent phosphorus as donor.

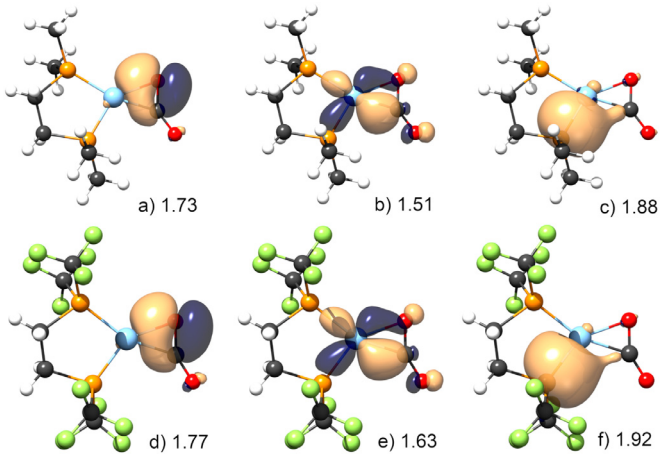

Fig. 6. DAFH eigenvectors with the corresponding eigenvalues for the donation (a, d), back donation (b, e), and bypassing back donating (c, f) interactions for complexes NiL(dmpe)(CO_2) (top) and NiL(dtfmpe)(CO_2) (bottom). Eigenvectors/eigenvalues a and b associated with CO_2 fragment whereas b, c, d, and e are associated with the Ni(diphosphine) fragment.

The selected eigenvectors with the corresponding eigenvalues are depicted in Fig. 6 for complexes NiL(dmpe)(CO_2) and NiL(dtfmpe)(CO_2). While the shapes of the electron pairs, by visual inspection, do not show noticeable differences, the eigenvalues are more informative regarding the electronic influence of the spectator ligand. In all cases, the three dominant donor-acceptor interactions are more polarized in the presence of dtfmpe. The donor pair is restricted to the carbon dioxide fragment by 88.5% for Ni(dtfmpe)(CO_2) whereas the percentage is 86.5% for Ni(dmpe)(CO_2). The pair from the bypassing back donation has a 6% contribution on the CO_2 fragments for Ni(dmpe)(CO_2) and this ratio drops to 4% in the case of Ni(dtfmpe)(CO_2). The difference is larger for the main back donating interaction: the pair, which stems mainly from the $d_{x^2-y^2}$ orbital of nickel, is shared by 24.5% : 75.5% and 18.5% : 81.5% between the CO_2 and the Ni(dmpe) fragments for Ni(dmpe)(CO_2) and Ni(dtfmpe)(CO_2), respectively.

The computed electronic parameters of diphosphines listed in Fig. 1 were determined according to Eq. (4) and compiled into Table 2 with the corresponding P-Ni-P bite angles. The chelating ligands were selected to address various geometrical as well as electronic parameters. Ligands **12**-**15** were used to illustrate the influence of the P-Ni-P bite angle upon the electronic structure of the coordinated CO_2 while ligands **16**-**19** show the effect of the substituents on the phosphorus with ethanediphos backbone. The chiral ligands **20**-**22** highlight the substituent effects on the ligand backbone. To address the structural changes of ligands with axial chirality **23**-**25** were chosen. Finally, **26** and **27** represent ligands possessing rigid structure with wide bite angles. In at-

Table 2
Computed asymmetric CO_2 stretching frequencies, P-M-P bite angles (θ_{PNiP} in degrees) for diphosphine containing complexes $NiL_2(CO_2)$, and their Computed Tolman Parameters (CEPs), determined according to Eq. 4. Vibrational frequencies are in cm^{-1}.

Ligand	$\nu(CO_2)$	$CEP_{NiL_2(CO_2)}$	θ_{PNiP}
dppm (**12**)	1849	2070	76.9
dppe (**13**)	1840	2068	90.8
dppp (**14**)	1837	2067	102.1
dppb (**15**)	1845	2069	109.6
dpm (**12H**)	n.a.	1909	75.8
dpe (**13H**)	n.a.	1900	90.3
dpp (**14H**)	n.a.	1893	99.5
dpb (**15H**)	n.a.	1894	104.0
dmpe (**16**)	1843	2069	91.6
dcpe (**17**)	1816	2062	91.8
dtbpe (**18**)	1819	2063	93.9
dtfmpe (**19**)	1967	2097	90.3
CHIRAPHOS (**20**)	1843	2069	91.0
BDPP (**21**)	1834	2067	101.4
DIOP (**22**)	1858	2072	105.8
BINAP (**23**)	1847	2070	102.0
BIPHEP (**24**)	1844	2069	103.0
SEGPHOS (**25**)	1840	2068	102.7
xantphos (**26**)	1851	2070	116.4
dppf (**27**)	1839	2068	109.2

tempt to separate the chelate effect from the steric bulk of the diphenylphosphino groups, a new set of ligands was taken into consideration, derived from dppm, dppe, dppp, and dppb where the phenyl groups on phosphorus were replaced by hydrogens and denoted as dpm (**12H**), dpe (**13H**), dpp (**14H**), and dpb (**15H**), respectively.

The CEPs obtained for $NiL_2(CO_2)$ complexes reveal close resemblance to those computed for carbonyl complexes $PdL_2(CO)$ and in most cases from those determined for the square planar carbonyl complexes $RhHL_2(CO)$ [55]. The largest difference is for the narrow bite angle dppm ligand (2070, 2073, and 2063 cm^{-1} for the nickel, palladium, and rhodium complex, respectively) and the large bite angle xantphos, where both carbonyl complexes show deviation (6 cm^{-1} for the Pd and 7 cm^{-1} for the Rh complex) from the Ni carbon dioxide complexes which could be explained by the larger bite angle calculated for Ni(xantphos)(CO_2)(116.4°) in comparison to that reported for Pd(xantphos)(CO) (105.9°). Nonetheless, the mean absolute deviation remains low: 2.4 cm^{-1} for the three coordinate Pd carbonyls and 3.2 cm^{-1} for the square planar rhodium hydrido carbonyl complexes.

Comparing CEPs of the $NiL_2(CO_2)$ complexes with ligands **12**–**15** provides information about the effect of the bite angle of the spectator diphosphine upon the back donation to the bound CO_2 while the basicity, determined by the substituents on both phosphorus atoms, remains the same. The increase of the bite angle by going in the direction of dppm →dppe →dppp results in a decrease in $\nu(CO_2)$, however, it is increased by 2 cm^{-1} by going from dppp to dppb. The change is noticeably larger for the simplified ligands: the difference in $\nu(CO_2)$ in Ni(**12H**)(CO_2) and Ni(**15H**)(CO_2) is 15 cm^{-1}.

Like for the carbonyl model compounds, the increase of basicity, by introducing methyl groups in the diphosphine backbone, results in negligable change in $\nu(CO_2)$ as it increases only 1 cm^{-1} when moving from dppe to CHIRAPHOS, and no change was obtained when dppp was replaced by BDPP. The complexes with ligands possessing axial chirality (**23**-**25**) show almost no difference in $\nu(CO_2)$ upon the presence or the structure of the condensed ring.

The coordination of CO_2 in the presence of ligands **12**-**19** was further examined utilizing the QTAIM methodology. Table 3 collects selected structural parameters as well as Ni-C and O1-C delocalization indices (δ) [56] and the O1–C bond ellipticities (ε). Ligands **12**-**15** are expected to have about the same basicity but they have different P-Ni-P bite angles. In terms of geometry, the bite angle seems to have almost no effect on the coordination strength of the CO_2 ligand. Bader parameters are also within a close range but they are little bit more subtle upon the geometry changes. The Ni-C interaction, followed by the delocalization index, is slightly stronger in the case of the 4-membered chelate ring and it decreases further upon increasing the ring size. The δ(O1,C) delocalization index is also somewhat larger for the dppm complex than that for the 5-, 6-, and 7-membered rings. The ellipticity of the O1–C bond showed a slight decrease by the increase of the ring size. The trend is very similar for the simplified ligands (**12H**-**15H**): the Ni–C bond is the strongest in Ni(**12H**)(CO_2), and shows a very slight increase from **13H** to **15H** with the increase of the bite angle. The coordinated CO_2 exhibits almost the same structural and electronic properties in the complexes with the four simplified ligands. Thus, it can be concluded that the electronic properties of the coordinated carbon dioxide are very insensitive upon the variation of the bite angle of the spectator chelating phosphine.

Notably larger variation can be obtained when the phenyl substituents are replaced by electron donating or electron withdrawing groups. The ligand dtbpe is known to promote the reduction of carbon dioxide to carbon monoxide while providing phosphine hemioxide [36] (see Fig. 2). Interestingly, among the basic diphosphines dmpe (**16**) does not cause a significant difference in the electronic structure of the Ni-CO_2 complex in comparison to that with dppe. In the presence of dcpe (**17**) and dtbpe (**18**), a higher reactivity of the coordinated CO_2 can be anticipated, according to shorter Ni-C and longer O1–Ni bonds and the smaller O1-C-O2 angles. The delocalization indices, which present the even more subtle differences regarding the bond strengths, reveal that the Ni-C interaction is somewhat stronger in Ni(**17**)(CO_2) than in Ni(**18**)(CO_2) (δ(Ni,C)=0.697, and 0.694, respectively, in contrast to δ(Ni,C)=0.679 in Ni(**13**)(CO_2)). On the other hand, the decrease of

Table 3
Structural and Bader parameters of complexes Ni(diphosphine)(CO_2).

Diphosphine	r(Ni-C) [Å]	r(O1-C) [Å]	∢O1-C-O2 [degree]	δ(Ni,C)	δ(O1,C)	ε(O1,C)
dppm (**12**)	1.884	1.270	142.2	0.694	1.163	0.067
dppe (**13**)	1.893	1.270	141.2	0.679	1.158	0.068
dppp (**14**)	1.893	1.269	141.2	0.676	1.157	0.066
dppb (**15**)	1.898	1.267	141.5	0.673	1.158	0.064
dpm (**12H**)	1.906	1.262	145.3	0.650	1.178	0.058
dpe (**13H**)	1.916	1.261	144.5	0.631	1.179	0.055
dpp (**14H**)	1.912	1.261	144.2	0.635	1.179	0.054
dpb (**15H**)	1.911	1.260	144.3	0.637	1.179	0.054
dmpe (**16**)	1.886	1.269	141.8	0.680	1.164	0.062
dcpe (**17**)	1.886	1.275	139.8	0.697	1.149	0.074
dtbpe (**18**)	1.887	1.274	140.0	0.694	1.151	0.072
dtfmpe (**19**)	1.967	1.251	148.2	0.546	1.201	0.041

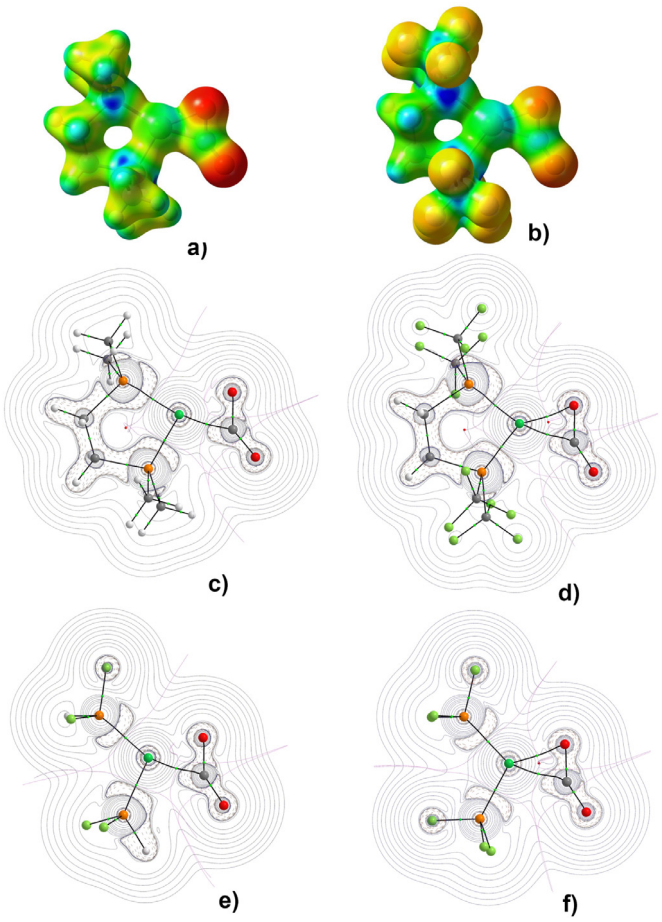

Fig. 7. Molecular electrostatic potentials (top) and Laplacians ($\nabla^2\rho$) of the electronic density (bottom) for complexes Ni(dmpe)(CO_2) and Ni(dtfmpe)(CO_2); Laplacians for complexes Ni(PF_2H)$_2$(CO_2) (e) and Ni(PF_3)$_2$(CO_2) (f).

δ(O1,C) shows a more activated C–O bond that is more susceptible to cleavage. The delocalization index is somewhat smaller for dcpe (1.149) than for dtbpe (1.151). The bond ellpticities are in line with the delocalization indices, as the somewhat higher values (0.074 and 0.072 for dcpe and dtbpe, respectively) indicate a slightly reduced bond order, moving from triple to double bond. As a comparison, δ(O1,C)=1.158, whereas ε(O1,C)=0.068 for dppe.

The electron withdrawing dtfmpe causes a clearly noticeable change in the electronic structure of bound CO_2. The Ni–C bond elongates whereas the O1–C bond is contracted and the bond angle of the coordinated carbon dioxide increases. The delocalization indices also suggest weaker CO_2 coordination in comparison to the other complexes with ethanediphos based ligands: δ(Ni,C) drops to 0.546, while δ(O1,C) increases to 1.201. The lower bond ellipticity (ε(O1,C)=0.041) suggests a somewhat higher triple bond character.

It was reported previously that in complex Ni(PF_3)$_2$(CO_2) no bond path was detected due to the excess of kinetic energy density in the vicinity of the Ni–O1 bond [53]. The same pattern was found if the nickel center was replaced by palladium or platinum [54]. Inspecting the Ni(PP)(CO_2) complexes with all the diphosphines, it was found that no bond path is formed between the O1 atom and the nickel center, in line with the previous results, except for dtfmpe (**19**). As shown in Table 2, ligand **19** has the highest CEP value; the difference is 28 cm^{-1} as compared to dmpe (**16**). The Laplacians of the electron density ($\nabla^2\rho$) with the bond paths for complexes Ni(dmpe)(CO_2) (**c**) and Ni(dtfmpe)(CO_2) (**d**) are depicted in Fig. 7. As a sharp contrast, a new O1–C bond path was obtained for Ni(dtfmpe)(CO_2) as a consequence of the reduced electron density around the Ni center. The molecular electrostatic potentials (MESPs) provide an appealing qualitative picture of the electron density distributions. In Ni(dmpe)(CO_2) the negative charge is strongly concentrated on the oxygen atoms (**a**), whereas the negative regions are more evenly distributed in the dtfmpe complex between the oxygens and the fluorines (**b**).

As a comparison, the topological analysis of the electron density for the phosphorus trifluoride complex Ni(PF_3)$_2$(CO_2) was completed as well and the same pattern of bond paths was observed as in the case of Ni(dtfmpe)(CO_2) (**f**) with a Ni-C and a Ni–O1 bond path. When one fluorine was replaced by hydrogen on both PF_3 ligands, the Ni–O1 bond path disappeared indicating that the bonding situation between the metal and the carbon dioxide ligand can be tuned by the introduction of electron withdrawing/donating groups.

4. Conclusion

In this paper, the electronic properties of the CO_2 ligand bound to nickel were investigated in $NiL_2(CO_2)$ model compounds employing the PBEPBE/def2-TZVP level of theory. The accomplishments of this work can be summarized as follows.

- Employing the training set used by Crabtree et al. in $Ni^{(0)}L_2(CO_2)$ complexes resulted in an acceptable linear correlation between the asymmetric stretching frequency of the bound CO_2 ligand and the Tolman's electronic parameters
- EDA-NOCV calculations show that back donation from the metal to CO_2 is the dominant part of the orbital interaction component.
- The orbital interaction energy, as well as the Hirshfeld charge related to back donation (ΔE^{π}_{bd} and qH^{π}_{bd}) show high linearity with the TEP scale.
- The computed electronic parameters for Ni(diphosphine)(CO_2) complexes show a reasonable agreement with those that had been obtained for model compounds $Pd^{(0)}L_2(CO)$ and $HRh^{(I)}L_2(CO)$.
- The size of the chelate ring has only a marginal effect upon the coordination properties of CO_2.
- When the substituents on the phosphorus atoms are changed from electron withdrawing to electron donating groups, the polarization of the electron pairs involved in the metal-ligand interactions decreases. Moreover, the strength of the nickel-carbon bond increases, whereas that of the O1–C bond decreases.
- For strongly electron withdrawing ligands, like dtfmpe or PF_3, two bond paths exist between the Ni center and the CO_2 ligand. Thus, the nickel complexes with these ligands reveal a different bonding pattern as compared to the other complexes in this study. When the electron withdrawing character decreases, the local negative charge accumulation around the coordinating oxygen start dominating that result in the disappearance of the Ni–O1 bond path.

Declaration of Competing Interest

The authors declare that they do not have any financial or non-financial conflict of interests.

Acknowledgments

This work has been supported by the GINOP-2.3.2-15-2016-00049 grant and the European Social Fund Grant no.: EFOP-3.6.1.-16-2016-00004 entitled by Comprehensive Development for Implementing Smart Specialization Strategies at the University of Pécs. The authors thank the Supercomputer Center of the National Information Infrastructure Development (NIIF) Program. GINOP is

the Hungarian Agency name, and it is incorporated in the grant number.

Appendix A. Supplementary material

Tables containing the internal energies and Cartesian coordinates of each species appearing in this study.

Supplementary material

Supplementary material associated with this article can be found, in the online version, at 10.1016/j.jorganchem.2020.121462.

References

[1] T. Sakakura, J.-C. Choi, H. Yasuda, Chem. Rev. 107 (2007) 2365–2387.
[2] I. Omae, Catal. Today 115 (2006) 33–52.
[3] M. Aresta, A. Dibenedetto, A. Dutta, Catal. Today 281 (2017) 345–351.
[4] M. Aresta, A. Dibenedetto, A. Angelini, J. CO2 Util. 3–4 (2013) 65–73.
[5] A. Álvarez, M. Borges, J.J. Corral-Pérez, J.G. Olcina, L. Hu, D. Cornu, R. Huang, D. Stoian, A. Urakawa, Chemphyschem 18 (2017) 3135–3141.
[6] E. Alper, O.Y. Orhan, Petroleum 3 (2017) 109–126.
[7] A. Paparo, J. Okuda, Coord. Chem. Rev. 334 (2017) 136–149.
[8] J. Mascetti, Carbon Dioxide Coordination Chemistry and Reactivity of Coordinated CO_2, John Wiley & Sons, Ltd, pp. 55–88.
[9] X. Yin, J.R. Moss, Coord. Chem. Rev. 181 (1999) 27–59.
[10] D.H. Gibson, Coord. Chem. Rev. 185186 (1999) 335355.
[11] J. Ma, N. Sun, X. Zhang, N. Zhao, F. Xiao, W. Wei, Y. Sun, Catal. Today 148 (2009) 221–231.
[12] M. Aresta, A. Dibenedetto, E. Quaranta, J. Catal. 343 (2016) 2–45.
[13] K.A. Grice, Coord. Chem. Rev. 336 (2017) 78–95.
[14] P. Gotico, Z. Halime, A. Aukauloo, Dalton Trans. 49 (2020) 2381–2396.
[15] C.M. Kozak, K. Ambrose, T.S. Anderson, Coord. Chem. Rev. 376 (2018) 565–587.
[16] R. Carrilho, L. Dias, R. Rivas, M. Pereira, C. Claver, A. Masdeu-Bultó, Catalysts 7 (2017) 210.
[17] Z. Ma, M.D. Porosoff, ACS Catal. 9 (2019) 2639–2656.
[18] W. Strohmeier, F.-J. Müller, Chem. Ber. 100 (9) (1967) 2812–2821.
[19] C.A. Tolman, J. Am. Chem. Soc. 92 (10) (1970) 2953–2956.
[20] C.A. Tolman, Chem. Rev. 77 (3) (1977) 313–348.
[21] O. Kühl, Coord. Chem. Rev. 249 (5) (2005) 693–704.
[22] W. Strohmeier, F.-J. Müller, Z. Naturforschg. 22b (1967) 451–452.
[23] D.R. Anton, R.H. Crabtree, Organometallics 2 (5) (1983) 621–627.
[24] A. Roodt, S. Otto, G. Steyl, Coord. Chem. Rev. 245 (1) (2003) 121–137.
[25] C.H. Suresh, N. Koga, Inorg. Chem. 41 (6) (2002) 1573–1578.
[26] H.Y. Liu, K. Eriks, A. Prock, W.P. Giering, Organometallics 9 (6) (1990) 1758–1766.
[27] J. Bartholomew, A.L. Fernandez, B.A. Lorsbach, M.R. Wilson, A. Prock, W.P. Giering, Organometallics 15 (1) (1996) 295–301.
[28] D.G. Gusev, Organometallics 28 (3) (2009) 763–770.
[29] M. Mitoraj, A. Michalak, Organometallics 26 (26) (2007) 6576–6580.
[30] M.P. Mitoraj, A. Michalak, Inorg. Chem. 49 (2) (2010) 578–582.
[31] T.R. Kégl, L. Kollár, T. Kégl, Adv. Chem. (2016) 4109758.
[32] E.P. Couzijn, Y.-Y. Lai, A. Limacher, P. Chen, Organometallics 36 (17) (2017) 3205–3214.
[33] L. Perrin, E. Clot, O. Eisenstein, J. Loch, R.H. Crabtree, Inorg. Chem. 40 (23) (2001) 5806–5811.
[34] D.A. Valyaev, R. Brousses, N. Lugan, I. Fernández, M.A. Sierra, Chem.–Eur. J. 17 (24) (2011) 6602–6605.
[35] G. Ciancaleoni, N. Scafuri, G. Bistoni, A. Macchioni, F. Tarantelli, D. Zuccaccia, L. Belpassi, Inorg. Chem. 53 (18) (2014) 9907–9916.
[36] J.S. Anderson, V.M. Iluc, G.L. Hillhouse, Inorg. Chem. 49 (2010) 10203–10207.
[37] M.J. Frisch, G.W. Trucks, H.B. Schlegel, G.E. Scuseria, M.A. Robb, J.R. Cheeseman, G. Scalmani, V. Barone, B. Mennucci, G.A. Petersson, H. Nakatsuji, M. Caricato, X. Li, H.P. Hratchian, A.F. Izmaylov, J. Bloino, G. Zheng, J.L. Sonnenberg, M. Hada, M. Ehara, K. Toyota, R. Fukuda, J. Hasegawa, M. Ishida, T. Nakajima, Y. Honda, O. Kitao, H. Nakai, T. Vreven, J.A. Montgomery Jr., J.E. Peralta, F. Ogliaro, M. Bearpark, J.J. Heyd, E. Brothers, K.N. Kudin, V.N. Staroverov, R. Kobayashi, J. Normand, K. Raghavachari, A. Rendell, J.C. Burant, S.S. Iyengar, J. Tomasi, M. Cossi, N. Rega, J.M. Millam, M. Klene, J.E. Knox, J.B. Cross, V. Bakken, C. Adamo, J. Jaramillo, R. Gomperts, R.E. Stratmann, O. Yazyev, A.J. Austin, R. Cammi, C. Pomelli, J.W. Ochterski, R.L. Martin, K. Morokuma, V.G. Zakrzewski, G.A. Voth, P. Salvador, J.J. Dannenberg, S. Dapprich, A.D. Daniels, O. Farkas, J.B. Foresman, J.V. Ortiz, J. Cioslowski, D.J. Fox, Gaussian 16 Revision C.01, Gaussian Inc. Wallingford CT, 2016.
[38] J.P. Perdew, K. Burke, M. Ernzerhof, Phys. Rev. Lett. 77 (1996) 3865–3868.
[39] F. Weigend, R. Ahlrichs, Phys.Chem.Chem.Phys. 7 (2005) 3297–3305.
[40] R.F.W. Bader, Atoms in Molecules - A Quantum Theory, Oxford University Press, Oxford, 1990.
[41] T.A. Keith, AIMAll (version 19.02.13), TK Gristmill Software, Overland Park KS, USA, (aim.tkgristmill.com), 2019.
[42] , ADF2019, SCM, Theoretical Chemistry, Vrije Universiteit, Amsterdam, The Netherlands, 2019.
[43] M. Mitoraj, A. Michalak, J. Mol. Model. 13 (2) (2007) 347–355.
[44] A. Michalak, M. Mitoraj, T. Ziegler, J. Phys. Chem. A 112 (9) (2008) 1933–1939.
[45] M.P. Mitoraj, A. Michalak, T. Ziegler, J. Chem. Theory Comput. 5 (4) (2009) 962–975.
[46] M.P. Mitoraj, H. Zhu, A. Michalak, T. Ziegler, Int. J. Quantum Chem. 109 (14) (2009) 3379–3386.
[47] R. Ponec, J. Math. Chem. 21 (3) (1997) 323–333.
[48] R. Ponec, J. Math. Chem. 23 (1–2) (1998) 85–103.
[49] R. Ponec, A.J. Duben, J. Comput. Chem. 20 (8) (1999) 760–771.
[50] R. Ponec, J. Roithová, Theor. Chem. Acc. 105 (4–5) (2001) 383–392.
[51] R. Ponec, G. Yuzhakov, M.R. Sundberg, J. Comput. Chem. 26 (5) (2005) 447–454.
[52] R. Ponec, G. Lendvay, J. Chaves, J. Comput. Chem. 29 (9) (2008) 1387–1398.
[53] T. Kégl, R. Ponec, L. Kollár, J. Phys. Chem. A 115 (45) (2011) 12463–12473.
[54] N. Pálinkás, L. Kollár, T. Kégl, ChemistrySelect 2 (20) (2017) 5740–5750.
[55] T. Kégl, N. Pálinkás, L. Kollár, T. Kégl, Molecules 23 (12) (2018) 3176.
[56] R.F.W. Bader, M.E. Stephens, J. Am. Chem. Soc. 97 (26) (1975) 7391–7399.